Urban Forestry & Urban Greening 124 (2026) 129580

Contents lists available at ScienceDirect

Urban Forestry & Urban Greening

journal homepage: www.elsevier.com/locate/ufug

Original article

Scalable urban tree canopy modelling for Canadian cities

Bayan F. Shaeri [a], Yuhao Lu [a,*], Alexander J.F. Martin [b,c], Lukas G. Olson [d], Raphael Ayambire [e], Txomin Hermosilla [f], Lucila M. Corro [g], Jay E. Diffendorfer [g], Peter C. Ibsen [g]

[a] Department of Landscape Architecture, Faculty of Architecture, University of Manitoba, 84 Curry Place, Winnipeg, MB R3T 2M6, Canada
[b] Department of Geography, Geomatics and Environment, University of Toronto Mississauga, 3359 Mississauga Road, Mississauga, ON L5L 1C6, Canada
[c] Doctoral Training Centre, University of Oxford, 1-4 Keble Rd, Oxford OX1 3NP, United Kingdom
[d] Department of Forest Resources Management, Faculty of Forestry, University of British Columbia, 2424 Main Mall, Vancouver, BC V6T 1Z4, Canada
[e] Department of City Planning, Faculty of Architecture, University of Manitoba, 84 Curry Place, Winnipeg, MB R3T 2M6, Canada
[f] Canadian Forest Service (Pacific Forestry Centre), Natural Resources Canada, 506 Burnside Road West, Victoria, BC V8Z 1M5, Canada
[g] U.S. Geological Survey, Geosciences and Environmental Change Science Center, Denver, CO 80225, USA

ARTICLE INFO

Keywords:
Green infrastructure
Random Forest regression
Remote sensing
Urban greenness
Urban forestry

ABSTRACT

Urban tree cover (UTC) is a key indicator for monitoring climate adaptation, guiding policy goals, and designing equitable cities. However, consistent UTC estimates remain limited. This study proposes a transferable UTC modelling framework using global open-source data to map fractional UTC. The method involves satellite spectral products and high-resolution canopy height data to build city-specific machine learning models of 19 Canadian cities. Model accuracy, assessed through cross-validation, ranged from $R^2 = 0.67–0.88$ with RMSE values of 5.5–16.3%. Independent validation against airborne laser scanning in three cities demonstrated strong agreement (Pearson $r = 0.82–0.92$). Results suggest that UTC distributions are unevenly distributed, typically right skewed, with large parks and riparian corridors accounting for a disproportionate share of UTC. Greenness and moisture are the most influential predictors, while model residuals concentrate in areas with higher UTC. The resulting UTC maps and modelling framework provide a consistent and reproducible framework for UTC distribution assessments, benchmarking across diverse ecozones, and monitoring UTC change at urban scales over time.

1. Introduction

Urban tree cover (UTC), measured as the percentage of an urban area covered by tree canopy (Konijnendijk, 2023), is a crucial metric in urban forest management and monitoring. UTC metrics are incorporated into urban planning documents through UTC targets among municipal governments and urban forestry organizations (Morgenroth et al., 2025). UTC datasets are also used in urban environmental research to examine topics like urban heat (Lu et al., 2022; Ziter et al., 2019), urban green accessibility (Locke et al., 2023; Martin & Conway, 2025), stormwater management (Selbig et al., 2022), air pollution reduction (Lovasi et al., 2013), wildlife movement ecology (Brunbjerg et al., 2018; Teixeira et al., 2013), and carbon storage accounting (Steenberg et al., 2023). Consistent UTC information therefore is necessary in baseline urban forest mapping and inventory, and monitoring progress towards future UTC targets.

UTC measures should be generated consistently, be spatially explicit, and be comparable across cities. More specifically, to fully assess UTC and establish benchmarks for urban forestry governance, planning, and research, UTC data and their modelling should be: (i) intuitive: expressing UTC as a percentage of urban land surface; (ii) spatially explicit: compatible with other geospatial modelling workflows; (iii) scalable: capable of producing repeated UTC estimates across large areas and over time; (iv) cost-effective: leveraging open-source and readily available datasets.

In the past, various approaches have been developed to collect, analyze, and represent urban trees at different scales (Miller et al., 2015). At the property and city block levels, canopy cover information (e.g., UTC) is often collected by hand-tracing canopies over aerial imagery (Martin, 2023). At such broader extents, UTC is more commonly estimated through manual photointerpretation of aerial imagery using models such as i-Tree (Nowak et al., 2018) or by sample plot estimates

* Corresponding author.
E-mail address: yuhao.lu@umanitoba.ca (Y. Lu).

https://doi.org/10.1016/j.ufug.2026.129580
Received 20 October 2025; Received in revised form 10 June 2026; Accepted 27 June 2026
Available online 29 June 2026
1618-8667/© 2026 The Authors. Published by Elsevier GmbH. This is an open access article under the CC BY license (http://creativecommons.org/licenses/by/4.0/).

using hemispherical photography (King and Locke, 2013), which require site visits and substantial sampling effort. Selim et al. (2023) recommended a photointerpretation sample point density of 760 samples per hectare (10,000 m^2), roughly equivalent to 1500 sample points per city block. These approaches can be time-consuming and labour-intensive when applied across broader spatial extents (i.e., at a city-wide level). Thus, there is a growing call for more systematic, scalable, and repeatable methods (Corro et al., 2025; Dong et al., 2025; Liu et al., 2024; Liu et al., 2024).

Recent progress in aerial and terrestrial laser scanning (ALS and TLS), as well as drone-based photogrammetry, enables such systematic production of datasets ranging from fine-scale, tree-level digital clones (Nitoslawski et al., 2019; Olson et al., 2025) to wall-to-wall maps of tree canopy locations (Erker et al., 2019). These techniques produce accurate 2D canopy delineations and 3D structural metrics, useful for building and validating large-extent, satellite-based inventories, by establishing statistical relationships between ALS- or TLS-based canopy metrics and spectral indicators from moderate-resolution imagery (Hermosilla et al., 2024). However, in urban contexts, municipal laser-scanning acquisition can be limited or temporally sparse or inconsistent, particularly in small communities.

Alternatively, UTC can also be estimated and mapped using spectral indices computed from medium-spatial-resolution multispectral imagery, such as the Landsat program, the Copernicus programme, and aerial imagery from the National Agriculture Imagery Program (NAIP). Despite the technical availability of satellite-derived vegetation indices, their uptake in planning practice remains limited in many cities (Martinez et al., 2023). While accessible through platforms such as Google Earth Engine (GEE; Gorelick et al., 2017), these indices, such as the normalized difference vegetation index (NDVI), can be difficult to interpret and not always intuitive for decision-makers (Feltynowski et al., 2018). Interpretable measures such as UTC provide additional quantification of urban trees for a variety of urban planning and research needs, particularly for small communities (Martinez et al., 2023).

In response to the need for open, scalable, and interpretable UTC data for large extents, global forest datasets have been developed, with a particular emphasis on canopy height models (CHMs) such as those by Lang et al. (2023) and Tolan et al. (2024). While these datasets represent significant advances in large-scale forest mapping, their application in urban environments remains limited. Similar to CHMs derived from ALS, these global CHM products provide complete high-resolution reference layers that support predictive model training and cross-validation (CV), thereby improving regional and local city-scale UTC modelling.

Conceptually, this modelling framework is positioned at the intersection of urban ecology, remote sensing, and overall urban sustainability and ecosystem services. Urban ecology provides the theoretical foundation, establishing UTC as a spatially explicit proxy for the provisioning of a wide range of ecosystem services in cities, including thermal regulation (Aminipouri et al., 2019), stormwater attenuation (Selbig et al., 2022), air quality improvement (Akbari et al., 2001), biodiversity support (Locke et al., 2023), and human well-being (Lafortezza et al., 2009), whose magnitude and distribution are fundamentally governed by the spatial configuration and density of UTC.

Urban remote sensing provides observations necessary to quantify UTC continuously, a capability that field-based inventory approaches cannot achieve at the city or multi-city scale (Galle et al., 2021; Lu et al., 2016; Nielsen et al., 2014). In addition, machine learning such as Random Forest (RF) regression (Breiman, 2001; Parmehr et al., 2016) provides the analytical bridge between multi-source spectral, thermal, and structural signals and the UTC estimates that urban ecology requires (Fassnacht et al., 2023).

Urban sustainability research further connects urban remote sensing and ecology by framing UTC distribution not only as a biophysical outcome but as a governance and fairness concern (Czekajlo et al., 2023; Nesbitt et al., 2017, 2019). The uneven spatial distribution revealed from modelling UTC reflects cumulative legacies of land-use planning, infrastructure investment, and socio-economic characteristics, with direct consequences for which communities benefit from canopy-mediated ecosystem services and which bear disproportionate exposure to urban heat, flooding, and poor air quality.

This conceptual position justifies the motivation for this study, the input datasets and variables used, and future research extending from it. This study makes three key contributions towards current UTC modelling. First, by harmonizing multi-source open data onto a moderate-resolution (120-m) grid, we mitigate the "salt-and-pepper" noise inherent in 30-m pixel classifications while retaining sufficient granularity for neighbourhood-level UTC research. Second, unlike municipal inventories that are often limited to street trees or public lands, this workflow provides wall-to-wall fractional UTC estimates across all land tenures, enabling a more holistic assessment of urban trees. Finally, by using globally available open-source datasets rather than local ALS data, we demonstrate a nationally applicable UTC modelling framework that can be applied to other Canadian cities. This method, tested across 19 Canadian cities of varying sizes, ecological settings, and built environments, can produce continuous, interpretable UTC percentages.

2. Methods

The method developed in this study integrates multi-source remote-sensing-derived variables, including spectral products, land-surface temperature, and built-form metrics. These variables were spatially harmonized using a 120-m grid system. We selected a 120-m analysis grid to capture intra-urban variation while reducing sensor-mismatch artifacts. This grid is equivalent to an area of 4 × 4 Landsat 30-m pixels and approximates the size of a typical city block (100–150 m) in Canada. By focusing on local calibration while ensuring national consistency, this approach provides a transferable basis for benchmarking UTC, evaluating urban canopy fairness, and reconstructing historical canopy trends from archived satellite imagery.

To account for local heterogeneity, we trained city-specific RF regression models with hyperparameters and a stratified CV scheme (Section 2.3). The method was applied and tested across 19 cities with varying urban ecological conditions found in eight Canadian ecozones. We validated model performance in two ways: first, through internal CV within the RF model to assess generalization and overfitting, and second, by comparing it against three independent sets of local ALS-derived UTC values (Section 2.4).

2.1. Study areas

The study involved 19 Canadian cities with diverse ecosystems, city-wide average UTCs, and city sizes (Fig. 1, Table 1). These cities are distributed across eight terrestrial ecozones (Terrestrial Ecozones of Canada - Open Government Portal, n.d), ranging from the Canadian Plant Hardiness Zone (Canada's Plant Hardiness Site | Natural Resources Canada, n.d) 1A (Thompson, MB) to 9 A (Vancouver, BC). UTC estimates derived from the Meta Canopy Height Model (CHM) ranged from 4% (Calgary, AB) to 54% (Prince George, BC) with a mean (μ) UTC of 22.5% (standard deviation σ = 13.4%).

Total urban area ranges from 17 km^2 (Thompson, MB) to 2788 km^2 (Ottawa, ON) ($\mu = 429$ km^2, $\sigma = 610.4$ km^2), based on the Canadian Census (Census Profile, 2021 Census of Population, n.d.). Thompson, MB, had the smallest population (13,035 residents), while Montréal, QC was the most populous (1,762,949 residents) ($\mu = 426{,}789$, $\sigma = 501{,}760$). Population densities range from 71 people per km^2 in Kenora, ON, to 5750 people per km^2 in Vancouver, BC ($\mu = 1178$, $\sigma = 1508.4$). Except for Thompson, MB, and Kenora, ON, all cities experienced population growth between 2016 and 2021, with an average increase of 4.86% ($\sigma = 3.94\%$).

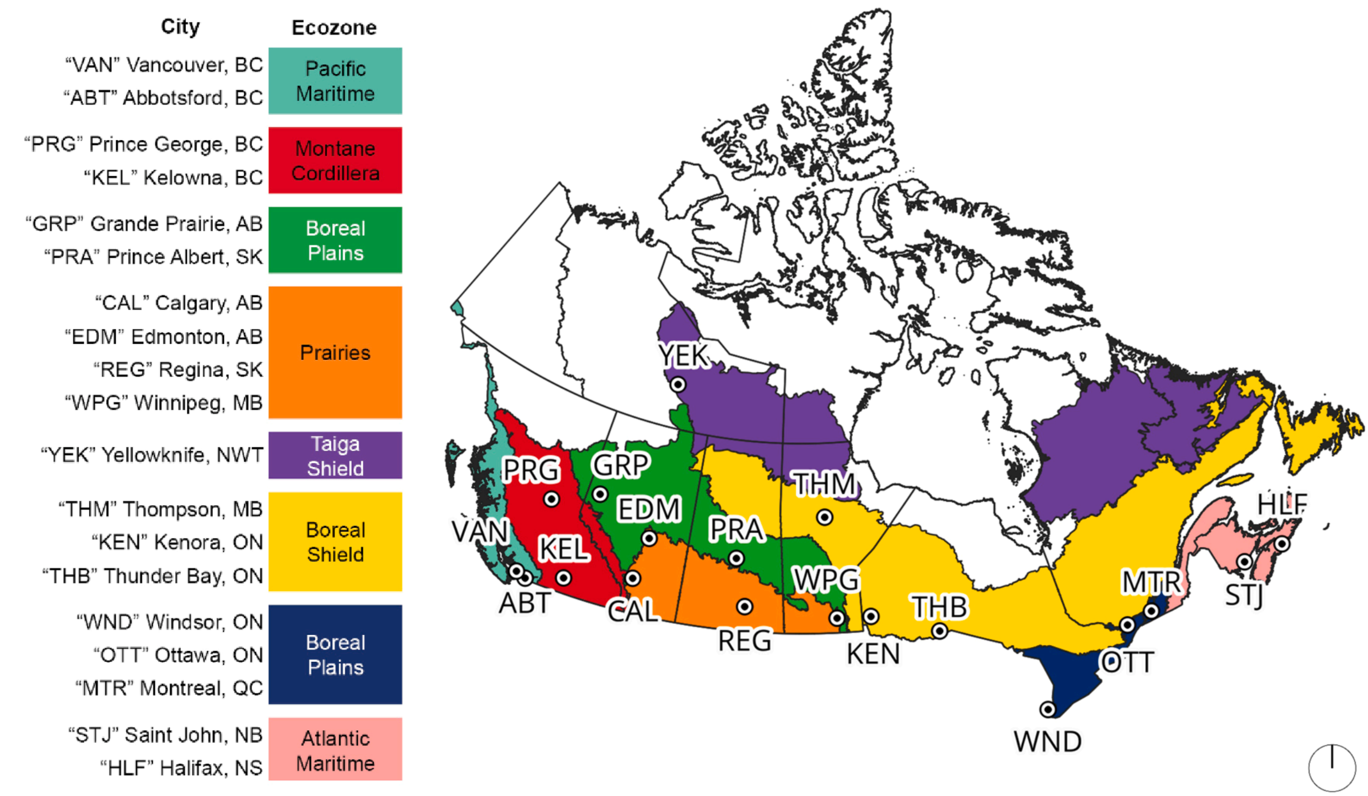

Fig. 1. Locations of the 19 study cities across eight terrestrial ecozones. The map is projected using EPSG: 4326.

Table 1
Population and climate of the 19 study cities, in order from westernmost to easternmost ecozones.

Study City, Prov	Ecozone	Area (km^2)	Pop. 2021 (x1000)	Pop. Change 2016–21 (%)	Pop. Density (/km^2)	Mean Annual Temp. (°C)	Mean Annual Precip. (mm)	Hardiness Zone
Vancouver, BC	Pacific Maritime	115	662	4.9	5750	10.5	1140	9A
Abbotsford, BC		375	153	8.6	409	10.7	1501	8B
Prince George, BC	Montane Cordillera	317	77	3.7	242	4.3	654	4B
Kelowna, BC		212	144	13.5	682	8.2	324	7A
Grande Prairie, AB	Boreal Plains	133	64	1.5	483	2.2	402	3A
Prince Albert, SK		67	38	5.1	562	1.4	85	2B
Calgary, AB	Prairies	821	1307	5.5	1592	4.5	554	4A
Edmonton, AB		766	1011	8.3	1320	2.4	499	4A
Regina, SK		179	226	5.3	1266	2.8	203	3A
Winnipeg, MB		462	750	6.3	1623	2.9	521	3B
Yellowknife, NWT	Taiga Shield	103	20	3.9	197	−4.0	283	1B
Thompson, MB	Boreal Shield	17	13	−4.7	784	−2.8	510	1A
Kenora, ON		212	15	−0.9	71	3.2	476	3B
Thunder Bay, ON		328	109	0.9	332	3.0	552	3B
Windsor, ON	Boreal Plains	146	230	5.7	1573	10.8	104	7B
Ottawa, ON		2788	1017	8.9	365	6.8	887	5A
Montréal, QC		365	1763	3.4	4833	7.0	1072	5B
Saint John, NB	Atlantic Maritime	316	70	3.4	221	5.3	923	5B
Halifax, NS		96	440	9.1	80	6.9	1148	6B

2.2. Model input datasets and variables

This study used three main datasets, namely the Landsat 8 Collection 2 Level 2 Surface Reflectance (30-m), the Global Human Settlement Layer (GHSL) harmonized datasets (100-m) for 2020 (Pesaresi and Politis, 2023a–c), and Meta-CHM (1-m) (Tolan et al., 2024). Landsat imagery was restricted to 2020 to maintain temporal alignment with the Meta CHM and GHSL reference datasets. Model input variables (Table S1, Supplementary Materials 1) were harmonised to a common 120-m grid prior to model fitting.

The combined use of spectral, thermal, and built-form predictors in RF model training is grounded in the complementary physical and ecological processes that govern urban tree canopy distribution and detectability. In addition, these datasets were selected because of their consistent spatial coverage and availability. This was an important consideration in this study because it made the method more transferable to cities not tested here. From these datasets, we computed 31 spectral indices (i.e., input variables) representing five sets of biophysical characteristics, namely greenness, moisture, brightness/soil, seasonal land surface temperature (LST), and built form. The aim is predictive accuracy rather than causal explanation. Therefore, we interpreted variable importance at the predictor-family level rather than at the individual-variable level.

Spectral indices, particularly vegetation indices, provide the primary signal of photosynthetically active vegetation through the differential reflectance of chlorophyll in the red and near-infrared wavelengths (Huete et al., 2002; Tucker, 1979). In this study, spectral indices on vegetation and moisture were derived from Landsat 8 Collection 2 Level 2 Surface Reflectance at a spatial resolution of 30 m. For each city, images were filtered only to include those acquired between June 1 and August 31, 2020. The selection of this time window corresponds to greatest availability of cloud-free Landsat scenes and more importantly the peak growing season across Canadian temperate and boreal urban environments. In this time frame, deciduous tree canopy reaches maximum foliar expression and spectral separability between vegetated and non-vegetated surfaces is greatest. To reduce noise and outlier values, a single image composite was created per city using all available scenes with a cloud cover of less than 10% (except for LST, where cloud cover greater than 30% in spring and 20% in summer was used to source cloudless scenes of each city).

LST derived from Landsat thermal bands, provide a complementary and physically independent signal. Tree canopy modifies the local thermal environment through evapotranspiration and shading, producing cooler surface temperatures in vegetated areas relative to surrounding impervious surfaces (Bowler et al., 2010; Locke et al., 2024; Ziter et al., 2019). LST was therefore derived from the Thermal Infrared Sensor (TIRS) Band 10 (resampled from 100-m to 30-m, USGS, 2019) from the Landsat 8 Collection 2 Level 2. LST values corresponded with two periods: spring (March 1 - May 31, 2020) and summer (June 1 - August 31, 2020). For cities that did not have LST scenes for 2020 below the cloud-cover threshold (10%), images from the same months in 2021 and 2022 (whichever year has the lowest cloud cover over the study area) were substituted. A total of six LST layers were derived for each city, including spring and summer minimum, maximum, and mean temperatures.

Built-form indicators, derived from the GHSL and related building layers, capture the structural context within which the canopy is embedded. Impervious surface areas, building height and volume influence both the physical space available for tree establishment and the microenvironmental conditions that determine canopy survival and growth (Dobbs et al., 2011; Nowak and Greenfield, 2018). GHSL was therefore used to characterize each city's built-up physical characteristics. For each grid cell, the following variables were calculated for building height (BH), volume (BV), and surface area (BS) using zonal statistics (mean, min, max, range, sum).

The primary spectral-index processing steps used to compute the input variables in Table S1 (Supplementary Materials 1), including Landsat surface reflectance retrieval, cloud masking, spectral-index calculation, and spatial aggregation, were conducted in GEE, with code provided in Supplementary Materials 2. All input variables were then further processed, projected to each city's UTM zone, and summarized on a 120-m grid with PyQGIS (Supplementary Materials 3).

Model training data were then derived from Meta's latest CHM (Tolan et al., 2024) (Fig. 2). To exclude turf, bushes, and shrubs, we filtered the CHM data using a minimum height threshold of 2 m (Ma et al., 2023). We then generated a binary canopy mask indicating whether canopy pixels exceeded 2 m within each grid cell. This sum was then divided by the total area of the grid and multiplied by 100 to determine each grid's UTC (%).

To standardize UTC modelling across all cities, we overlaid a 120-m grid for each city. This grid size was selected to support the aggregation of variables derived from datasets with different spatial resolutions, such as spectral indices (30-m) and building data (100-m), while remaining fine enough to distinguish neighbourhood characteristics. City boundaries were sourced from the GADM dataset (GADM database of Global Administrative Areas, 2022). Grid cells intersecting city boundary lines (i.e., at the edges of each city) were excluded to maintain dimensional uniformity with the other grid cells.

2.3. *Urban Tree Cover Modelling*

The workflow described in this section (Fig. 3) was developed and

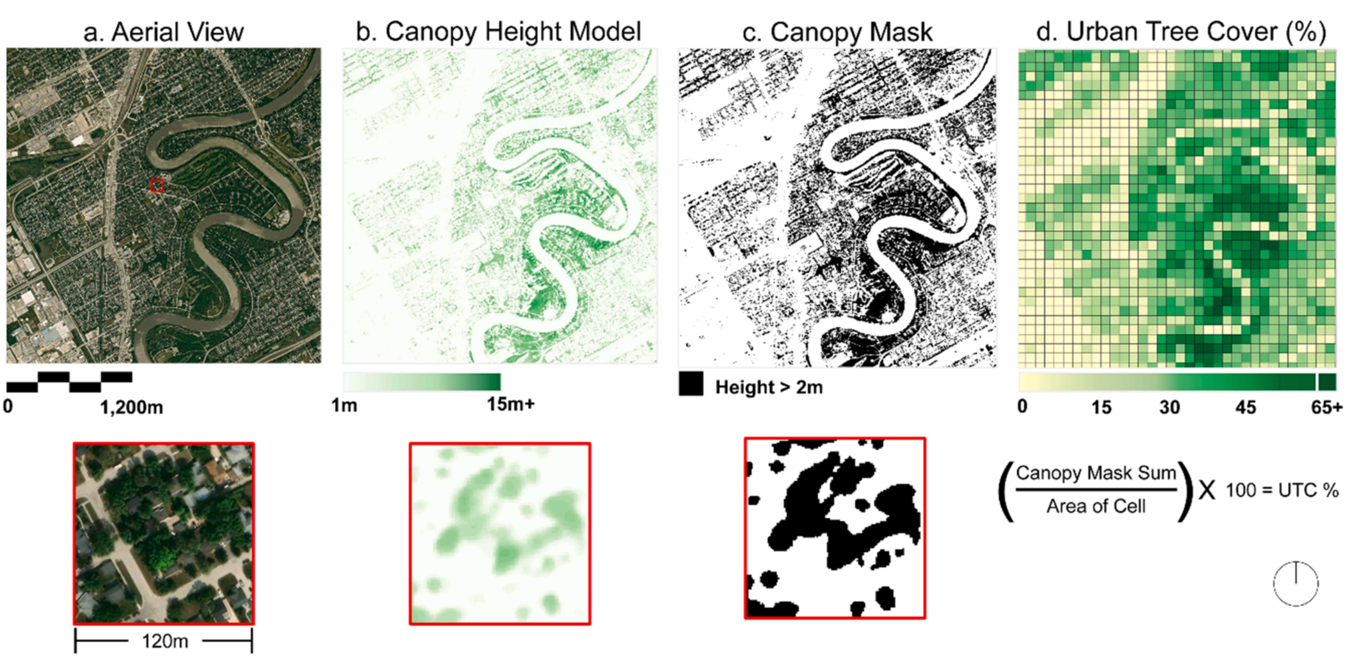

Fig. 2. Procedure for calculating urban tree cover (UTC) from the canopy height model data: (a) aerial view used as spatial reference, (b) filtered canopy height model data, (c) binary canopy mask applied to filter canopy pixels, and converted into a (d) UTC percentage for each grid cell. These maps are from Winnipeg, MB, Canada to illustrate the key steps. All maps are projected to EPSG: 32614 (UTM Zone 14 N).

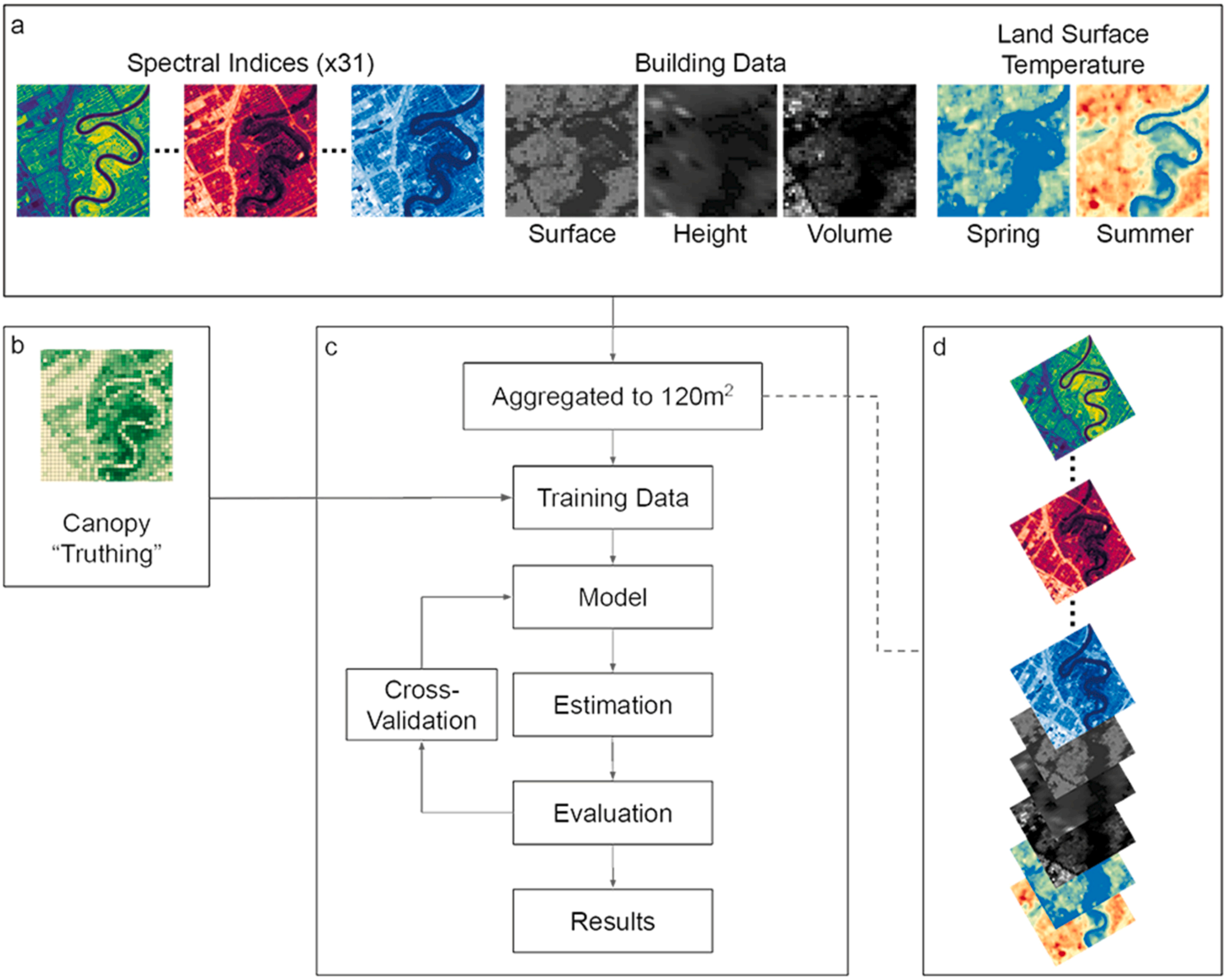

Fig. 3. Workflow diagram of inputs into the Random Forest regression model. Input datasets (spectral indices, building data, and LST) were aggregated into a 120-m grid. Box a represents all input raster datasets from Landsat and GHSL; Box b represents the UTC derived from Meta's CHM, which will be used in Box c for model training and cross-validation. Box d depicts the 120-m aggregation step using all inputs from Box and canopy data from Box b. Exemplary maps (EPSG: 32614) represent the city of Winnipeg, MB, Canada.

initially tested on a consumer-level desktop computer, then scaled to a high-performance computing environment via Compute Canada for processing all 19 cities. Critically, aggregating predictions to a 120-m grid rather than pixel-level 30-m classification substantially reduces computational demand, making the workflow tractable on standard municipal computing infrastructure.

RF regression is an ensemble method that trains multiple decorrelated decision trees on bootstrap-resampled data, with random feature subsampling at each split, and averages their predictions to improve accuracy and reduce overfitting (Breiman, 2001). The RF was implemented in R using *ranger* (Wright and Ziegler, 2017). Each model was trained independently to estimate UTC from aggregated spectral indices, LST, and building data, using a 120-m grid.

CV was implemented using 30-fold stratified partitioning, which assigned observations to folds based on quantiles of the response variable. This ensured that each fold contains a representative distribution of UTC values across the full UTC range. To reduce heteroscedasticity introduced by the skewed distribution of UTC percentages, we first normalized the UTC values using a natural logarithm transformation. Model estimates were then back-transformed and converted to percentages, with zero UTC values left unchanged throughout the process.

Seven RF model parameters were defined following established parameterization from prior studies (Hermosilla et al., 2024; Mulverhill et al., 2024), namely, CV folds, number of decision trees, feature importance, number of variables sampled at each split, minimum node size, proportion of data sampled per tree, and splitting criteria (Supplementary Material 1, Table S2)

Variable importance scores in each RF model were obtained from each CV fold and averaged across all 30 folds to calculate a mean importance percentage for each predictor variable. Given the expected collinearity among spectral predictors, variable importance may be distributed arbitrarily across correlated variables rather than highlighting the most meaningful ones (Strobl et al., 2008). Thus, variables were grouped by input category to emphasize the overall significance and frequency of each group. This is to mitigate high multicollinearity among the input variables, which can affect the reliability of individual variable importance rankings.

2.4. Model performance and accuracy

Robustness to spatial dependence was enforced via spatially blocked, stratified 30-fold CV with non-overlapping test grids. To capture predictive accuracy and error magnitude relative to observed UTC values, model performance was assessed using R^2, root mean squared error (RMSE) and mean absolute error (MAE). In addition, three cities (Vancouver, Ottawa, and Winnipeg) were used to perform a secondary independent validation against their respective local ALS dataset.

3. Results

3.1. Model performance and accuracy

The spatial distribution of residuals across the 19 study cities revealed consistent within-city patterning despite considerable variation in overall error magnitude (RMSE: 5.5–16.3%; MAE: 2.6–10.8%). Residuals were generally centred around zero across all cities, indicating low overall systematic bias at the city level. These findings were further reflected in the approximately symmetric histograms of residuals.

CV yielded an average R^2 of 0.80, ranging from 0.67 (Kelowna, BC) to 0.88 (Prince George, BC). A higher R^2 was observed in cities with a wide range of UTC values (i.e., spanning both low and high UTC values). In contrast, lower R^2 values were attained in areas where UTC is more uniformly low or moderate.

Spatially, underestimation of UTC (green in Fig. 4) was consistently concentrated in high-UTC areas, such as urban parks, forest patches, and riparian buffers, while overestimation (red in Fig. 4) tended to occur in transitional and mixed urban-vegetation zones. Cities with low average UTC, such as Calgary (RMSE: 6.8%), Regina (RMSE: 5.5%), and Edmonton (RMSE: 8.6%), produced the lowest errors overall. Conversely, Thompson (RMSE: 16.3%) and Montréal (RMSE: 15.2%) had the highest error rates. Notably, Vancouver and Windsor deviated from the general pattern, exhibiting comparatively low error rates despite high average UTC values among these 19 cities.

Residual scatterplots across the 19 study cities (Fig. 5) revealed structural statistical error patterns that reflect both the distributional properties of UTC and inherent constraints of the RF regression framework. Residuals were broadly centred around zero across all cities, confirming low overall systematic bias at the city level, consistent with the RMSE and MAE values reported in Fig. 4. However, the statistical spread of residuals was not uniform in Fig. 5. Cities with high average UTC and a greater proportion of densely vegetated UTC grids (e.g., Prince George, Saint John, Thunder Bay, and Ottawa) exhibited substantially wider residual distributions, particularly in the low-to-mid predicted UTC range (0–40%), where positive residuals indicated systematic underestimation of actual canopy cover calculated from Meta's CHMs.

In contrast, cities with overall low UTC, such as Calgary and Regina, exhibited tightly constrained residuals, concentrated near zero across the predicted UTC range, reflecting the model's stronger performance when predictions fall within a narrower, more evenly distributed range. Thompson, the smallest of all study cities, is a notable outlier, exhibiting the widest and most dispersed residual spread of all cities (i.e., the highest RMSE, 16.3%), consistent with the coarser spatial heterogeneity of its land cover and the limited training sample size given the city's extent.

Notably, Montreal exhibited a distinct pattern relative to other high-UTC cities, with its residuals tightly clustered at low predicted values but widening considerably in the mid-range (20–50% predicted UTC), indicating that model uncertainty was concentrated in transitional urban-vegetation zones rather than in the densest canopy areas.

Independent validation compared the RF-estimated UTC against ALS-derived UTC in Vancouver, BC; Winnipeg, MB; and Ottawa, ON (Fig. 6). The correlation between the two ranged from 0.82 to 0.92. Winnipeg, MB, shows the lowest correlation ($r = 0.82$) with reduced agreement at higher UTC (50% and above). Vancouver, BC, had a correlation of $r = 0.90$, and Ottawa, ON, the largest city in the sample with the broadest UTC distribution, had the highest correlation ($r = 0.92$).

3.2. Importance of model predictors

Spectral indices consistently ranked highly across all models (Fig. 7). The Atmospherically Resistant Vegetation Index (ARVI) was the most frequently identified variable. It was ranked in the top 20 most important variables in 16 (out of 19) cities. The spring minimum LST had the highest median importance weight among all predictors, despite influencing only two models (Grande Prairie, AB, and Abbotsford, BC). Brightness and soil metrics, along with seasonal composites, contributed to minor but consistent improvements in model performance, especially in cities located in open or semi-arid environments.

Further analysis of variable importance by ecozone revealed distinct patterns (Supplementary Material 1, Figure S1). The Atlantic Maritime and Boreal Shield ecozones, both known for their extensive forest cover, exhibited high importance scores for greenness and wetness variables. The Tasselled Cap Wetness index and building height consistently ranked in the top 20 variables for cities in the Prairies, despite their wide range of importance scores: building height values between 5 and 35, and Tasselled Cap Wetness values between 2 and 32. Vegetation indices, such as NDVI and enhanced vegetation index (EVI), were ranked more consistently across all ecozones, although their median importance scores remained relatively low.

3.3. Fractional UTC maps of 19 Canadian cities

Fig. 8 revealed the city-specific spatial distribution of UTC. In most cities, UTC were strongly right skewed, with many grids having little or no canopy, while a smaller share of grids accounts for high UTC values (> 65%). This skewness resulted in relatively low medians occurring in several cities such as Calgary, AB; Regina, SK; and Grande Prairie, AB.

Cities with expansive park systems or forest reserves (top row of Fig. 8), as expected, exhibited a higher proportion of UTC over 65%. In contrast, those dominated by cropland (bottom row of Fig. 8) displayed a substantially lower average city-wide UTC value. This was also evident in the statistical distribution of UTC values. Within each city, contiguous high-UTC patches matched large urban park systems like Stanley Park in Vancouver, BC; Hemlock Ravine Park in Halifax, NS; and Mount Royal Park in Montréal, QC, as well as riparian corridors such as the Seine River in Winnipeg, MB, and the North Saskatchewan River in Edmonton, AB.

Cities tested in this study also exhibited a UTC gradient, with moderate UTC in established residential neighbourhoods transitioning to low UTC in the urban peripheries. For example, neighbourhoods on the west side of Vancouver, BC, tend to be more treed than those in the east while neighbourhoods along major riverways in Edmonton, AB, and Winnipeg, MB, are noticeably greener than other parts of the city. In several instances, such as Regina, SK, and Windsor, ON, the estimated UTC also reveals the street tree planting patterns and block structure, even at a 120-m grid scale.

All estimated UTC datasets of these 19 cities are available as GeoJSON files at https://object-arbutus.cloud.computecanada.ca/webMaps/canTrees/canUTC.html.

4. Discussion

4.1. UTC mapping model performance

RF models achieved accuracy comparable to recent regional fractional tree cover models. Corro et al. (2025) reported an average R^2 of 0.75 and RMSE ranging from 24.7% in a regional-wide UTC (30-m spatial resolution) estimation modelling procedure for US cities. At a coarser spatial resolution (500 m), Liu et al. (2024) estimated a global forest fraction with an R^2 of 0.73 when validated against the circa 2010 USGS global land cover reference dataset. At finer spatial resolutions, Erker et al. (2019) reported a MAE of 6% at the city-block level, which matches the average MAE (6%) observed in our model.

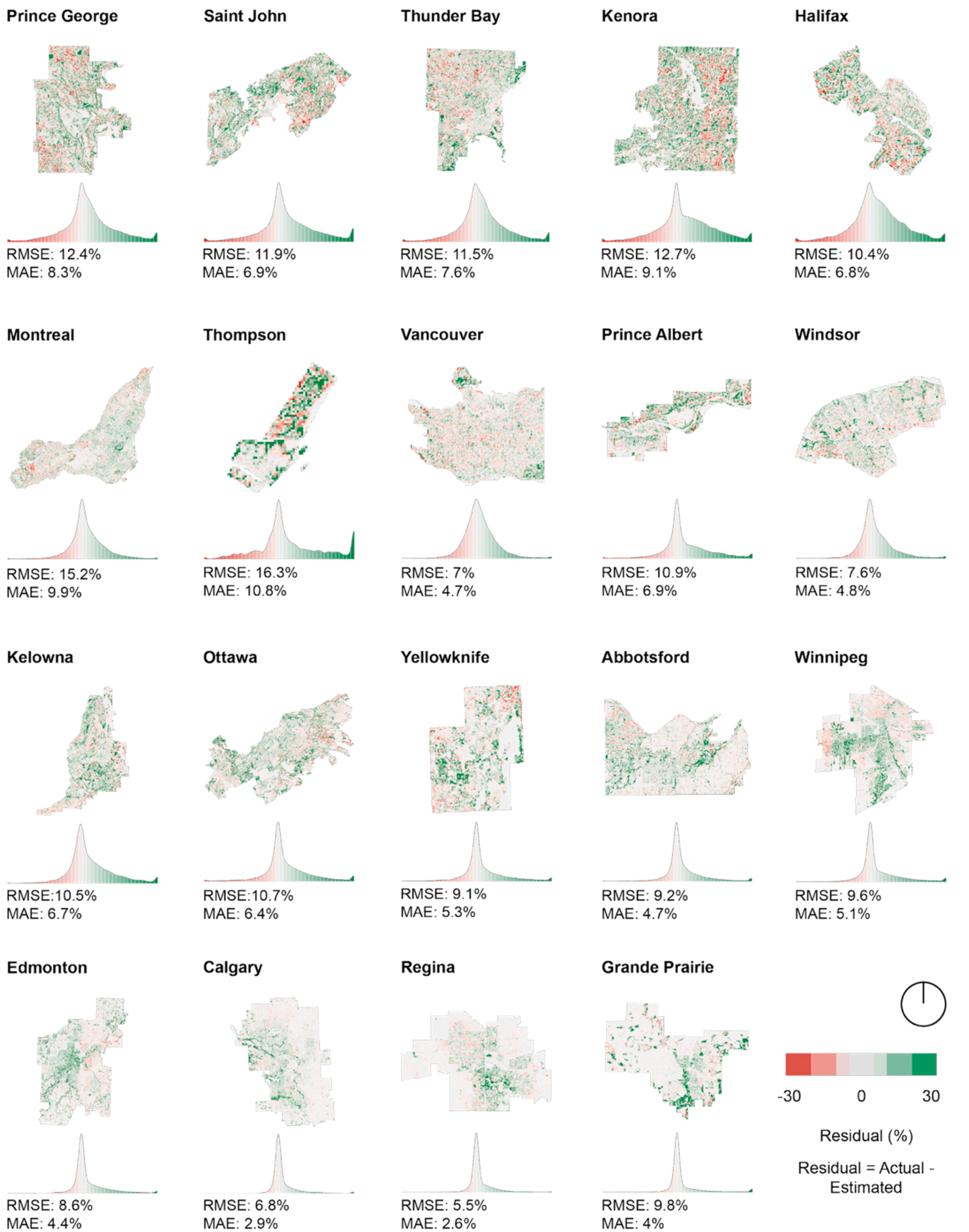

Fig. 4. Grid-level UTC residuals with histograms of spatial residual errors for each grid, alongside city-level root mean squared error (RMSE) and mean absolute error (MAE). Green indicates underestimation, while red shows overestimation in urban tree cover. Cities are arranged from highest UTC median values to the lowest. Maps are projected using their respective UTM zones.

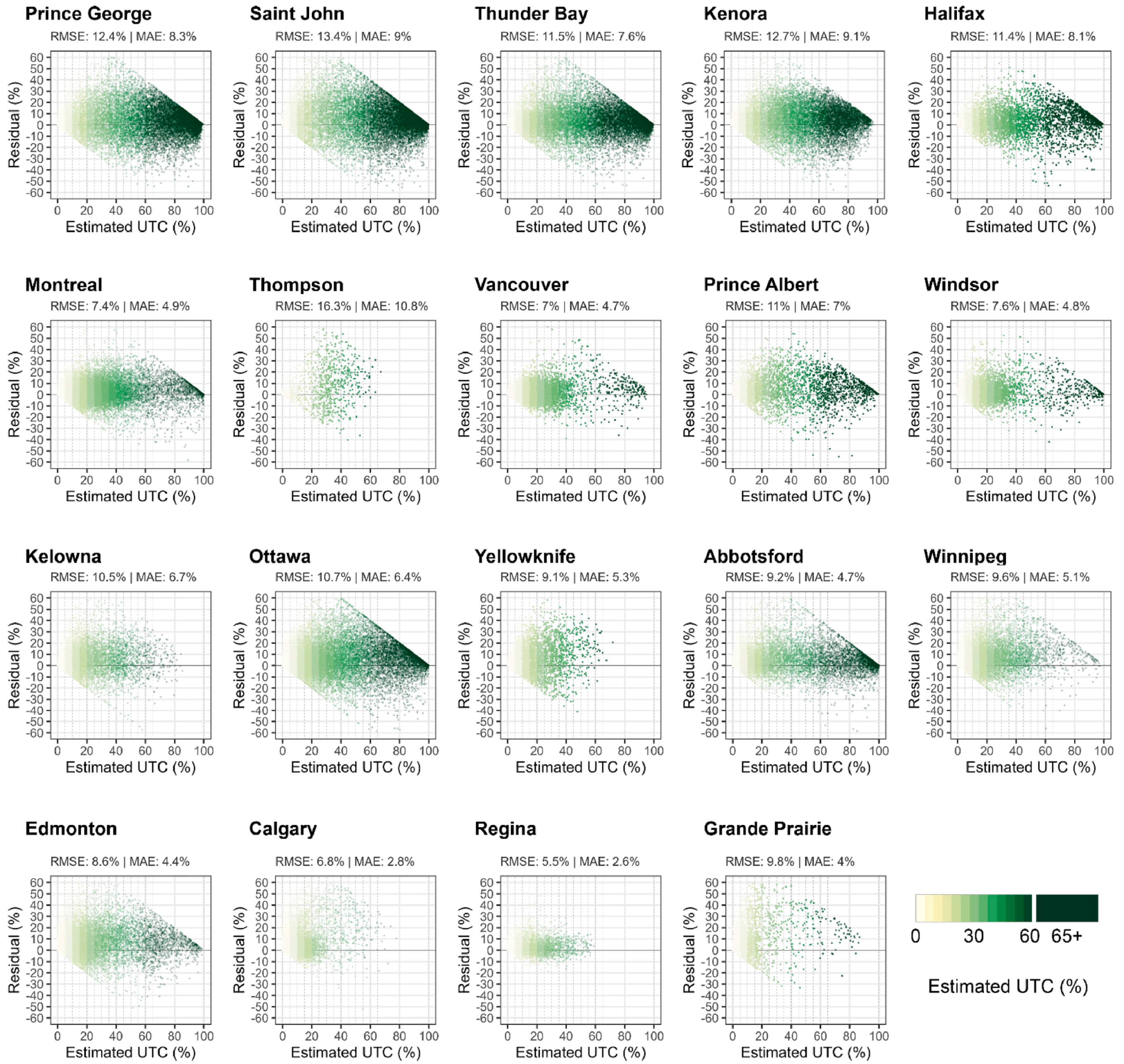

Fig. 5. Residual plots for 19 Canadian cities. Each panel shows the relationship between estimated Urban Tree Canopy (UTC) on the x-axis and the residual (Meta CHM-derived UTC minus Estimated UTC) on the y-axis for each city. Points are coloured by estimated UTC range. The solid horizontal line at zero indicates perfect prediction. Diagonal lines represent the theoretical upper and lower residual boundaries imposed by the physical constraint that UTC values are bounded between 0% and 100%. Each panel subtitle reports the Root Mean Square Error (RMSE) and Mean Absolute Error (MAE) for that city. The widening residual spread at low-to-mid predicted UTC values and compression toward zero at high predicted UTC values are consistent with the known tendency of Random Forest regression to underestimate extreme UTC values due to its averaging mechanism, compounded by spectral saturation of optical inputs at high canopy densities.

Differences in model performance and variable importance across ecozones indicate underlying biophysical conditions and urbanization patterns across Canada. Forested ecozones yielded stronger model fits, likely due to greater canopy variability and less extreme right-skew in UTC distributions. In contrast, the uniformly sparse canopy characteristics in the Prairies are more difficult to estimate using spectrally derived variables (Martin et al., 2025a). The results of this study also suggest evidence that ecological and climate contexts might influence local UTC potential and RF model behaviour. This finding implies that municipal UTC targets and policy expectations should be ecozone-specific. For example, “high UTC” targets appropriate for cites in Atlantic Maritime ecozone would be unrealistic in the Prairies.

We also found that UTC underestimation in densely treed areas is spatially clustered (in large urban forests or along riparian forests) and accounts for only a fraction of the land area in most cities included in this study. This is important to acknowledge because RF regression models cannot extrapolate beyond their training range, meaning that there were few grids at high UTC, and the model tends to regress towards the mean. This could lead to an overall underestimation of UTC in very dense canopy areas. Future research can conduct a Moran’s I analysis (Moran, 1950; Schindler and Schindler, 2025) on the residual maps to distinguish between spatially random prediction error and structured spatial bias concentrated in specific canopy density ranges. In addition, Quantile Regression Forests (Meinshausen, 2006) could also

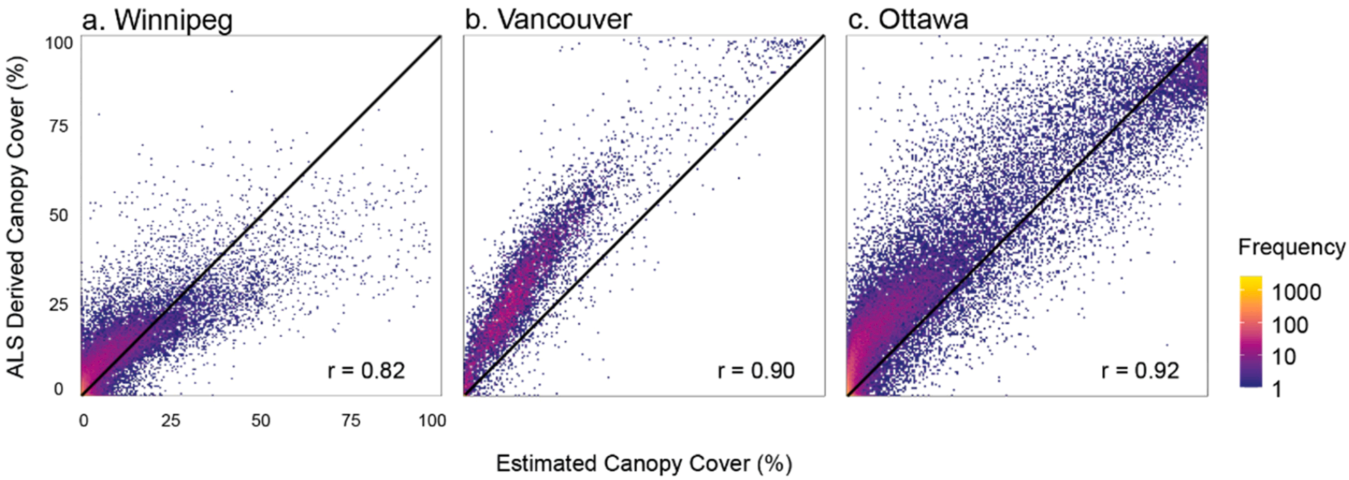

Fig. 6. Validation of our estimated UTC against airborne laser scanning-derived UTC for three study cities: a. Winnipeg, MB; b. Vancouver, BC; and c. Ottawa, ON. The panels show binned-frequency scatterplots, with colours indicating point density. Pearson correlation (r) and a 1:1 line is included for each city.

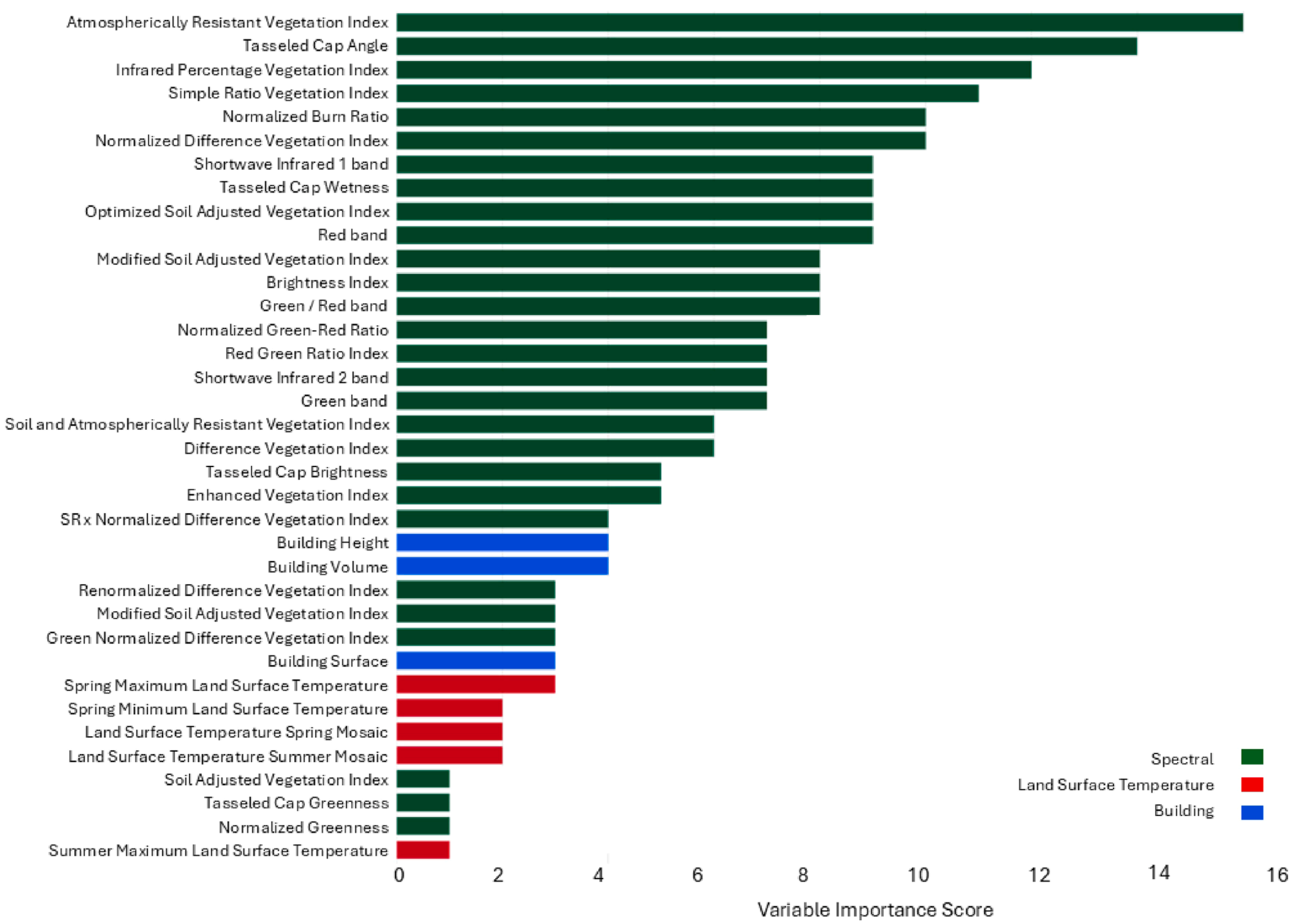

Fig. 7. Variables ranked by frequency (i.e., the number of times a variable was ranked in the top 20 per model) of importance in the UTC models, coloured by variable category.

be implemented in future work to provide pixel-level prediction intervals that explicitly quantify uncertainty as a function of canopy density, offering a more nuanced uncertainty characterization than city-level RMSE.

Moreover, underestimation in high-UTC areas likely reflects the well-documented saturation of broadband optical indices, which were used extensively as predictors. At high canopy densities, spectral response plateaus and the model lose discriminative signal precisely in the range where accurate prediction matters most (Mutanga and Skidmore, 2004). As mentioned above, this is compounded by an inherent property of RF regression: its averaging mechanism compresses predictions toward the training mean, systematically underestimating

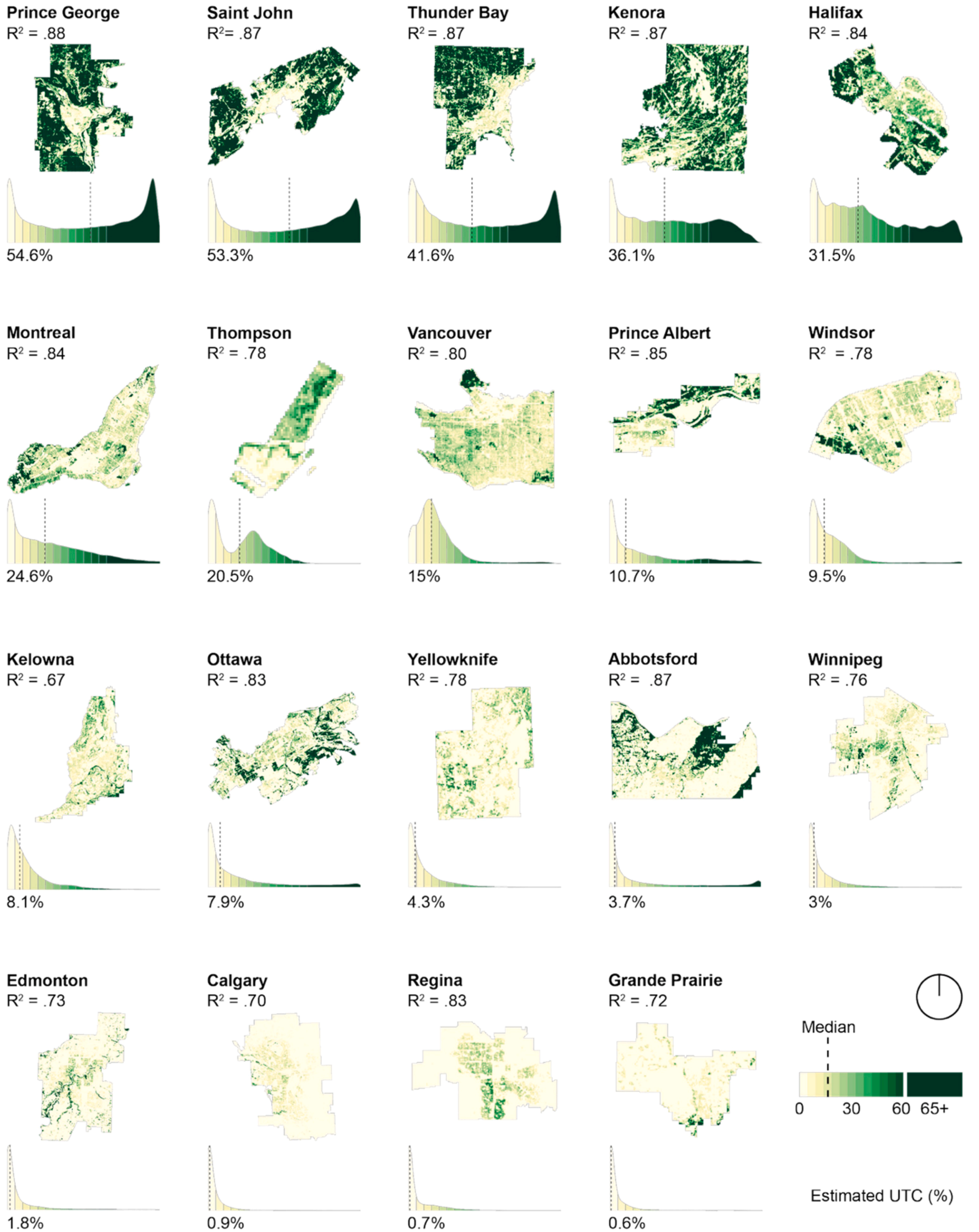

Fig. 8. Grid-level UTC map and histogram of UTC values. Each panel shows a grid-level UTC map (light to dark green represents low to high UTC values) with an aligned histogram of grid UTC values. The dotted line marks the city median UTC. All maps share the same colour scale (continuous from 0% to 60%, and a single colour for UTC over 65%). Cities are arranged from the highest UTC to the lowest. Maps are projected using their corresponding UTM zones.

extremely high values regardless of input feature quality (Zhang and Lu, 2012).

At the same time, the contrasting pattern of overestimation in transitional urban-vegetation areas likely reflects spectral confusion among partial canopy cover, impervious surface shadows, and true canopy, a known limitation of passive optical sensors in heterogeneous urban environments (Lu et al., 2017). Together, these mechanisms explain why low-UTC cities such as Calgary and Regina achieved the lowest error: their models rarely operate at distribution extremes in either direction, avoiding both saturation and compression effects. The case of Montréal (high R^2 but elevated RMSE) is also instructive, as it shows that rank-order accuracy (R^2) and magnitude accuracy (RMSE) are distinct and should be used together when evaluating model performance.

Lastly, variable rankings from each model indicate which predictors were "universally" helpful for predicting UTC and should therefore be prioritized in future UTC models. Indices that reflect vegetation "greenness" were the most influential in the model across all cities (Fig. 7). This indicates that canopy cover is best captured by indices sensitive to chlorophyll and leaf area (Haboudane et al., 2002). Moisture-related indices such as Tasseled Cap Wetness and short-wave infrared combinations also improved the overall UTC estimation (Houseman et al., 2023; Vogeler et al., 2018), highlighting the role of canopy water content and understory moisture in distinguishing treed from non-treed areas. Models that combine greenness and moisture features effectively capture these gradients, yielding higher R^2 values and lower overall residuals.

4.2. Future model improvement and research opportunities

The proposed UTC modelling method can be improved in several complementary ways. Landsat imagery as the primary input, as discussed earlier with respect to residual patterns, may limit accuracy in spectrally heterogeneous high-UTC areas. The performance of multispectral Sentinel−2 imagery (10-m) remains untested. We hypothesize that higher-resolution inputs would reduce mixed-pixel effects, especially in transitional urban-vegetation zones, potentially addressing part of the overestimation bias observed in Figs. 4 and 5. Additionally, the spatial-resolution sensitivity analysis is a meaningful direction for future research.

Input features could also be enhanced via time-series embeddings generated by pre-trained large-scale deep learning models for semantic feature extraction (e.g., Google's AlphaEarth; Brown et al., 2025; Tollefson, 2025). Such representations could capture finer-resolution textures, context, and morphology beyond those captured by spectral indices. However, it is worth noting that the use of image embeddings may reduce model interpretability compared to traditional regression models (Rudin, 2019), potentially limiting their uptake in management-oriented applications.

While the overall accuracy of Tolan's CHM dataset was reportedly high for mapping forest height (Tolan et al., 2024), its reliability in complex urban environments remains an open research question. While Dong et al. (2025) conducted a recent study across four cities in the USA, Tolan's CHM performance in Canadian cities remains uninvestigated. Moreover, Tolan's CHM tends to overestimate the tree height of lower (0–5 m) canopy height ranges (Dong et al., 2025). This could lead to an overestimation of our UTC values used in model training and CV, since our canopy mask was generated using CHM greater than 2 m.

Models could also be strengthened by incorporating detailed intra-city-level land-use and land-cover data for Canada. Corro et al. (2025) used the moderate-resolution National Land Cover Database (NLCD) for US cities. However, NLCD is not available for Canadian cities. The Dynamic World LULC (Brown et al., 2022) provides 10 m global coverage, yet its capacity to distinguish fine-scale urban land-cover types remains limited. By examining the Dynamic World dataset via its web interface (https://dynamicworld.app/explore), we found that despite its high spatial resolution (10 m) and extensive coverage (global scale), the dataset's ability to map intra-urban LULC variations is rather limited. At least from a visual assessment of the data, the majority of land-use and land-cover classes within a city are classified as "Built-Up Area", even in areas known to have large parks and visible urban tree cover.

While city-specific RF models may introduce local biases, this is a necessary trade-off to achieve higher accuracy for each city than for a "one-size-fits-all" national model of all Canadian cities. We also acknowledge that independent validation in this study was limited to three cities (Vancouver, Winnipeg, Ottawa) due to the scarcity of open-access airborne laser scanning (ALS) data across Canada. With the release of high-resolution digital surface and terrain models (DSM and DTM) from Natural Resources Canada (NRCAN, 2025), the models proposed in this study can be further validated using more cities.

Similarly, since socio-economic variables are often found to be correlated with UTC distribution in cities (Neckerman et al., 2009; Nesbitt et al., 2019), incorporating such variables could potentially improve overall model performance while also offering evidence to inform research on the distributional fairness of UTC (Ayambire and Moos, 2024; Chuang et al., 2017; Zhao and Gong, 2024). Future analyses could include socio-economic variables from census data disaggregated to a spatial resolution consistent with the grid-based framework introduced in this study.

4.3. Urban tree canopy in Canadian cities: patterns and implications

The UTC model proposed in this study complements local municipal inventories by providing spatially explicit UTC estimates across all land tenures. Because municipal inventories include mostly street trees, often excluding trees in private, park, and riparian lands. This limits the generalizability of analyses based solely on street tree populations. UTC modelled from this study captures parks, woodlands, riparian areas, and private trees that are typically omitted from municipal tree inventories in Canada. In addition, recent work by (Martin et al., 2025a) synthesized public tree inventories from 32 Canadian cities to evaluate the distributional fairness of urban trees. The UTC products developed herein enable further research for Martin et al. (2025) by providing wall-to-wall maps of fractional canopy estimates that support both inter- and intra-city assessments of distributional fairness (e.g., linking UTC with income, heat exposure, and development era). This study thus offers a consistent modelling method for estimating and comparing UTC among Canadian cities.

Using a grid-based analysis with remote sensing imagery data, this UTC model provides greater spatial detail than recent fractional canopy products, such as GLOBMAP FTC, at a 250-m spatial resolution (Liu, et al., 2024). Our modelling approach provides comprehensive and temporally consistent UTC estimates that complement existing city tree inventories. Although local city inventories provide detailed information on species composition and maintenance (e.g., pruning schedules, tree health), this remote sensing-based UTC modelling method offers spatially continuous coverage and enables repeatable monitoring of UTC over time across all land tenures.

Regular and repeated UTC measurements are critical for assessing UTC targets (Nowak and Greenfield, 2018; Steenberg et al., 2023), establishing ecozone-specific benchmarks (Morgenroth et al., 2025), and evaluating the effectiveness of tree-protection bylaws and policies (Martin et al., 2025b). The fractional UTC workflow enables cities, even those without high-resolution ALS data, to construct UTC time series at approximately five-year intervals, aligning with the update frequency of GHSL dataset.

A nationwide UTC modelling framework thus has direct consequences for policy implications. Urban forestry targets expressed as absolute percentage thresholds (e.g., the widely cited 30% canopy cover target) (Nowak and Greenfield, 2018) may be systematically underreported in already-green cities, paradoxically penalizing cities that are closest to meeting canopy goals. Conversely, overestimation in transitional zones may inflate perceived progress in cities undergoing active greening, where the new canopy is patchy and spectrally mixed with surrounding surfaces. Cities like Vancouver and Windsor, which achieved low errors despite high UTC, may represent cases where the canopy is spatially homogeneous enough to avoid these extremes, suggesting that canopy spatial configuration, not just overall coverage, is a meaningful predictor of UTC model reliability.

In addition, we acknowledge that the spatial patterns of UTC and their associated prediction errors reported here may also partly reflect the legacy of differential urban investment, neighbourhood-level urban tree management styles, capacity, and land-use zoning. This contextualizes the model's outputs within the broader socio-spatial processes that shape urban forest distribution, without compromising the methodological independence of the UTC estimates themselves.

5. Conclusion

This study presents a standardized and transferable UTC modelling framework for mapping fractional tree covers in Canadian cities using exclusively open-source datasets. By integrating the Global Human Settlement Layer (GHSL), Meta’s Canopy Height Model (CHM), and Landsat spectral indices on a 120-m grid, we bridged the operational gap in UTC mapping between resource-intensive local ALS inventories and global forest products. We tested this method across 19 Canadian cities, achieving cross-validated R^2 between 0.67 and 0.88, and high agreement with independent ALS datasets (Pearson $r = 0.82$–0.92) in three cities. Results suggest that while "greenness" and "moisture" predictors are universally important, model performance varies by ecozones. Forested regions yield higher accuracy, whereas the sparse, discontinuous canopies of Prairie cities present greater spectral challenges. We also observed that model residuals tend to cluster in high-UTC areas (e.g., riparian corridors), likely reflecting the spectral saturation limitations inherent to optical sensors in dense canopies. This UTC democratizes access to consistent, wall-to-wall urban canopy data. Because the inputs are globally available, this framework allows municipalities, regardless of their ability to fund repeated ALS missions, to generate reliable baselines for monitoring UTC in climate adaptation and analyzing its distributional fairness. Future research direction includes further examining the spatial distribution of RF residuals, investigating the potential UTC implications in the distributional fairness of UTC in cities, and building a time series (5-year interval) of UTC datasets.

CRediT authorship contribution statement

Ibsen Peter C.: Writing – review & editing. **Diffendorfer Jay E.:** Writing – review & editing. **Martin Alexander J. F.:** Writing – review & editing, Validation, Conceptualization. **Yuhao Lu:** Writing – review & editing, Writing – original draft, Validation, Supervision, Software, Resources, Project administration, Methodology, Investigation, Funding acquisition, Data curation, Conceptualization. **Shaeri Bayan Furutan:** Writing – review & editing, Writing – original draft, Visualization, Validation, Methodology, Investigation, Formal analysis, Data curation. **Corro Lucila M.:** Writing – review & editing, Conceptualization. **Txomin Hermosilla:** Writing – review & editing, Visualization, Supervision, Conceptualization. **Raphael Ayambire:** Writing – review & editing, Conceptualization. **Lukas G. Olson:** Writing – review & editing, Methodology.

Declaration of Competing Interest

The authors declare that they have no known competing financial interests or personal relationships that could have appeared to influence the work reported in this paper.

Acknowledgements

We thank the University of Manitoba’s URGP and URA for supporting funding for this research. We also thank the University of Manitoba Grex High Performance Computing Centre (RRID: SCR_026342) for providing computing support and cloud storage. Additionally, we thank Dr. Nicholas Coops for his valuable comments on the early draft of this manuscript. Any use of trade, firm, or product names is for descriptive purposes only and does not imply endorsement by the U.S. Government.

Appendix A. Supporting information

Supplementary data associated with this article can be found in the online version at doi:10.1016/j.ufug.2026.129580.

References

Akbari, H., Pomerantz, M., Taha, H., 2001. Cool surfaces and shade trees to reduce energy use and improve air quality in urban areas. Sol. Energy 70 (3), 295–310. https://doi.org/10.1016/S0038-092X(00)00089-X.

Aminipouri, M., Rayner, D., Lindberg, F., Thorsson, S., Knudby, A.J., Zickfeld, K., Middel, A., Krayenhoff, E.S., 2019. Urban tree planting to maintain outdoor thermal comfort under climate change: The case of Vancouver’s local climate zones. Build. Environ. 158, 226–236. https://doi.org/10.1016/j.buildenv.2019.05.022.

Ayambire, R.A., Moos, M., 2024. Inclusive Futures? A Systematic Review of Social Equity in Scenario Planning. J. Plan. Educ. Res. https://doi.org/10.1177/0739456X241238684.

Bowler, D.E., Buyung-Ali, L., Knight, T.M., Pullin, A.S., 2010. Urban greening to cool towns and cities: A systematic review of the empirical evidence. In: Landscape and Urban Planning, 97. Elsevier, pp. 147–155. https://doi.org/10.1016/j.landurbplan.2010.05.006.

Breiman, L., 2001. Random forests. Mach. Learn. 45 (1), 5–32. https://doi.org/10.1023/A:1010933404324.

Brown, C.F., Brumby, S.P., Guzder-Williams, B., Birch, T., Hyde, S.B., Mazzariello, J., Czerwinski, W., Pasquarella, V.J., Haertel, R., Ilyushchenko, S., Schwehr, K., Weisse, M., Stolle, F., Hanson, C., Guinan, O., Moore, R., Tait, A.M., 2022. Dynamic World, Near real-time global 10 m land use land cover mapping. Sci. Data 9 (1), 1–17. https://doi.org/10.1038/s41597-022-01307-4.

Brown, C.F., Kazmierski, M.R., Pasquarella, V.J., Rucklidge, W.J., Samsikova, M., Zhang, C., Shelhamer, E., Lahera, E., Wiles, O., Ilyushchenko, S., Gorelick, N., Lydia Zhang, L., Alj, S., Schechter, E., Askay, S., Guinan, O., Moore, R., Boukouvalas, A., Kohli, P., DeepMind, G., 2025. Alpha Found. Embed. Field Model. accurate Effic. Glob. Mapp. sparse Label. data. ⟨https://arxiv.org/pdf/2507.22291⟩.

Brunbjerg, A.K., Hale, J.D., Bates, A.J., Fowler, R.E., Rosenfeld, E.J., Sadler, J.P., 2018. Can patterns of urban biodiversity be predicted using simple measures of green infrastructure? Urban. For. & Urban. Green. 32, 143–153. https://doi.org/10.1016/J.UFUG.2018.03.015.

Canada’s Plant Hardiness Site | Natural Resources Canada. (n.d.). Retrieved August 13, 2025, from ⟨https://planthardiness.gc.ca/?lang=en&m=22⟩.

Census Profile, 2021 Census of Population. (n.d.). Retrieved August 24, 2025, from ⟨https://www12.statcan.gc.ca/census-recensement/2021/dp-pd/prof/index.cfm?Lang=E⟩.

Chuang, W.C., Boone, C.G., Locke, D.H., Grove, J.M., Whitmer, A., Buckley, G., Zhang, S., 2017. Tree canopy change and neighborhood stability: A comparative analysis of Washington, D.C. and Baltimore, MD. Urban. For. & Urban. Green. 27, 363–372. https://doi.org/10.1016/J.UFUG.2017.03.030.

Corro, L.M., Bagstad, K.J., Heris, M.P., Ibsen, P.C., Schleeweis, K.G., Diffendorfer, J.E., Troy, A., Megown, K., O’Neil-Dunne, J.P.M., 2025. An enhanced national-scale urban tree canopy cover dataset for the United States. Sci. Data 12 (1), 490. https://doi.org/10.1038/s41597-025-04816-0.

Czekajlo, A., Cheng, Z., Barron, S., Girling, C., Nesbitt, L., 2023. Modelling Four Neighbourhood-Scale Urban Forest Scenarios for 2050: Vancouver, Canada. Arboric. & Urban. For. (AUF) 50 (1), 18–56. https://doi.org/10.48044/JAUF.2023.025.

Dobbs, C., Escobedo, F.J., Zipperer, W.C., 2011. A framework for developing urban forest ecosystem services and goods indicators. Landsc. Urban. Plan. 99 (3–4), 196–206. https://doi.org/10.1016/j.landurbplan.2010.11.004.

Dong, H., Xu, Z., Wu, J., Lan, T., Wang, L., Shao, G., Tang, L., 2025. High-precision airborne LiDAR remains essential for urban forestry: Revealing the limitations of recent large-scale canopy height products in urban contexts. Int. J. Appl. Earth Obs. Geoinf. 143. https://doi.org/10.1016/j.jag.2025.104791.

Dong, W., Yuan, H., Lin, W., Liu, Z., Xiang, J., Wei, Z., Li, L., Li, Q., Dai, Y., 2025. A global urban tree leaf area index dataset for urban climate modeling. Sci. Data 12 (1), 1–12. https://doi.org/10.1038/s41597-025-04729-y.

Erker, T., Wang, L., Lorentz, L., Stoltman, A., Townsend, P.A., 2019. A statewide urban tree canopy mapping method. Remote. Sens. Environ. 229, 148–158. https://doi.org/10.1016/J.RSE.2019.03.037.

Fassnacht, F.E., White, J.C., Wulder, M.A., Naesset, E., 2023. Remote sensing in forestry: current challenges, considerations and directions. For. Int. J. For. Res. 2023, 1–27. https://doi.org/10.1093/FORESTRY/CPAD024.

Feltynowski, M., Kronenberg, J., Bergier, T., Kabisch, N., Łaszkiewicz, E., Strohbach, M. W., 2018. Challenges of urban green space management in the face of using inadequate data. Urban. For. & Urban. Green. 31, 56–66. https://doi.org/10.1016/J.UFUG.2017.12.003.

GADM database of Global Administrative Areas. (2022). ⟨https://gadm.org/index.html⟩.

Galle, N.J., Halpern, D., Nitoslawski, S., Duarte, F., Ratti, C., Pilla, F., 2021. Mapping the diversity of street tree inventories across eight cities internationally using open data. Urban. For. & Urban. Green. 61, 127099. https://doi.org/10.1016/j.ufug.2021.127099.
Gorelick, N., Hancher, M., Dixon, M., Ilyushchenko, S., Thau, D., Moore, R., 2017. Google Earth Engine: Planetary-scale geospatial analysis for everyone. Remote sensing of Environment 202, 18–27.
Haboudane, D., Miller, J.R., Tremblay, N., Zarco-Tejada, P.J., Dextraze, L., 2002. Integrated narrow-band vegetation indices for prediction of crop chlorophyll content for application to precision agriculture. Remote. Sens. Environ. 81 (2–3), 416–426. https://doi.org/10.1016/S0034-4257(02)00018-4.
Hermosilla, T., Wulder, M.A., White, J.C., Coops, N.C., Bater, C.W., Hobart, G.W., 2024. Characterizing long-term tree species dynamics in Canada's forested ecosystems using annual time series remote sensing data. For. Ecol. Manag. 572, 122313. https://doi.org/10.1016/J.FORECO.2024.122313.
Houseman, I., Schleeweis, K., Heyer, J., Ruefenacht, B., Bender, S., Megown, K., Goetz, W., Bogle, S., 2023. Natl. Land. Cover. Database TreeCanopy Cover. Methods.
Huete, a, Didan, K., Miura, T., Rodriguez, E.P., Gao, X., Ferreira, L.G., 2002. Overview of the radiometric and biophysical performance of the MODIS vegetation indices. Remote. Sens. Environ. 83 (1–2), 195–213. https://doi.org/10.1016/S0034-4257(02)00096-2.
King, K.L., Locke, D.H., 2013. A Comparison of Three Methods for Measuring Local Urban Tree Canopy Cover. Arboric. & Urban. For. (AUF) 39 (2), 62–67. https://doi.org/10.48044/JAUF.2013.009.
Konijnendijk, C.C., 2023. Evidence-based guidelines for greener, healthier, more resilient neighbourhoods: Introducing the 3–30–300 rule. J. For. Res. 34 (3), 821–830. https://doi.org/10.1007/s11676-022-01523-z.
Lafortezza, R., Carrus, G., Sanesi, G., Davies, C., 2009. Benefits and well-being perceived by people visiting green spaces in periods of heat stress. Urban. For. Urban. Green. 8 (2), 97–108. https://doi.org/10.1016/j.ufug.2009.02.003.
Lang, N., Jetz, W., Schindler, K., Wegner, J.D., 2023. A high-resolution canopy height model of the Earth. Nat. Ecol. Evol. 7 (11), 1778–1789. https://doi.org/10.1038/S41559-023-02206-6.
Liu, Y., Liu, R., Chen, J., Wei, X., Qi, L., Zhao, L., 2024. A global annual fractional tree cover dataset during 2000–2021 generated from realigned MODIS seasonal data. Sci. Data 11 (1), 1–13. https://doi.org/10.1038/S41597-024-03671-9.
Liu, Y., Liu, R., Qi, L., Chen, J., Dong, J., Wei, X., 2024. Global mapping of fractional tree cover for forest cover change analysis. ISPRS J. Photogramm. Remote. Sens. 211, 67–82. https://doi.org/10.1016/J.ISPRSJPRS.2024.03.019.
Locke, D.H., Baker, M., Alonzo, M., Yang, Y., Ziter, C.D., Murphy-Dunning, C., O'Neil-Dunne, J.P.M., 2024. Variation the in relationship between urban tree canopy and air temperature reduction under a range of daily weather conditions. Heliyon 10 (3), e25041. https://doi.org/10.1016/j.heliyon.2024.e25041.
Locke, D.H., Grove, Morgan, Pickett, J., 2023. The Role of Urban Tree Canopies in Environmental Justice and Conserving Biodiversity. S. T. A. https://doi.org/10.1093/oso/9780198877271.003.0006.
Lovasi, G.S., O'Neil-Dunne, J.P.M., Lu, J.W.T., Sheehan, D., Perzanowski, M.S., Macfaden, S.W., King, K.L., Matte, T., Miller, R.L., Hoepner, L.A., Perera, F.P., Rundle, A., 2013. Urban tree canopy and asthma, wheeze, rhinitis, and allergic sensitization to tree pollen in a New York city birth cohort. Environ. Health Perspect. 121 (4), 494–500. https://doi.org/10.1289/EHP.1205513.
Lu, Y., Coops, N.C., Hermosilla, T., 2016. Regional assessment of pan-Pacific urban environments over 25 years using annual gap free Landsat data. Int. J. Appl. Earth Obs. Geoinf. 50, 198–210. https://doi.org/10.1016/j.jag.2016.03.013.
Lu, Y., Coops, N.C., Hermosilla, T., 2017. Estimating urban vegetation fraction across 25 cities in pan-Pacific using Landsat time series data. ISPRS J. Photogramm. Remote. Sens. 126, 11–23. https://doi.org/10.1016/j.isprsjprs.2016.12.014.
Lu, Y., McCarty, J., Sezto, J., Cheng, Z., Martino, N., Girling, C., Rysanek, A., Barron, S., Matasci, G., 2022. Modeling the Shading Effect of Vancouver's Urban Tree Canopy in Relation to Neighborhood Variations. Arboric. & Urban. For. (AUF) 48 (2), 95–112. https://doi.org/10.48044/JAUF.2022.008.
Ma, Q., Lin, J., Ju, Y., Li, W., Liang, L., Guo, Q., 2023. Individual structure mapping over six million trees for New York City USA. *10:1* Sci. Data 2023 10 (1), 1–12. https://doi.org/10.1038/s41597-023-02000-w.
Martin, A.J.F., 2023. Hutterite colonies and canopy cover: A remotely sensed analysis of the effects of cultural-religious beliefs on the treed landscape. Trees For. People 14, 100423. https://doi.org/10.1016/J.TFP.2023.100423.
Martin, A.J.F., Conway, T.M., 2025. Using the Gini Index to quantify urban green inequality: A systematic review and recommended reporting standards. Landsc. Urban. Plan. 254, 105231. https://doi.org/10.1016/J.LANDURBPLAN.2024.105231.
Martin, A.J.F., Fleming, A., Conway, T.M., 2025a. Distributional inequities in tree density, size, and species diversity in 32 Canadian cities. *Npj Urban.* Sustainability 5 (1), 1–10. https://doi.org/10.1038/S42949-025-00210-2.
Martin, A.J.F., Fleming, A., Conway, T.M., 2025b. Protecting trees in the urban forest: a systematic review of literature on acts, bylaws, ordinances, and regulations, 33. https://doi.org/10.1139/ER-2024-0118. ⟨Https://Doi.Org/10.1139/Er-2024-0118⟩.
Martinez, A., de la, I., Labib, S.M., 2023. Demystifying normalized difference vegetation index (NDVI) for greenness exposure assessments and policy interventions in urban greening. Environ. Res. 220, 115155. https://doi.org/10.1016/J.ENVRES.2022.115155.
Meinshausen, N., 2006. Quantile Regression Forests. J. Mach. Learn. Res. 7, 983–999.
Miller, R.W., Hauer, R.J., Werner, L.P., 2015. planning and managing urban greenspaces. Urban forestry. Waveland Press, Inc.
Moran, P.A.P., 1950. Notes on Continuous Stochastic Phenomena. Biometrika 37 (1/2), 17. https://doi.org/10.2307/2332142.
Morgenroth, J., Doick, K., Hauer, R., Locke, D.H., Barona, C.O., Roman, L.A., Conway, T. M., Dobbs, C., Duinker, P., Gulsrud, N.M., Jim, C.Y., Koeser, A.K., Landry, S., Livesley, S., Nesbitt, L., Shackleton, C.M., Tan, P.Y., Yang, J., 2025. Urban Tree Cover Targets: The good, the bad and the SMART. Urban. For. & Urban. Green., 128979 https://doi.org/10.1016/J.UFUG.2025.128979.
Mulverhill, C., Coops, N.C., Wulder, M.A., White, J.C., Hermosilla, T., Bater, C.W., 2024. Multidecadal mapping of status and trends in annual burn probability over Canada's forested ecosystems. ISPRS J. Photogramm. Remote. Sens. 209, 279–295. https://doi.org/10.1016/J.ISPRSJPRS.2024.02.006.
Mutanga, O., Skidmore, A.K., 2004. Narrow band vegetation indices overcome the saturation problem in biomass estimation. Int. J. Remote. Sens. 25 (19), 3999–4014. https://doi.org/10.1080/01431160310001654923.
Neckerman, K.M., Lovasi, G.S., Davies, S., Purciel, M., Quinn, J., Feder, E., Raghunath, N., Wasserman, B., Rundle, A., 2009. Disparities in Urban Neighborhood Conditions: Evidence from GIS Measures and Field Observation in New York City. J. Public. Health Policy 30 (1), S264–S285. https://doi.org/10.1057/jphp.2008.47.
Nesbitt, L., Hotte, N., Barron, S., Cowan, J., Sheppard, S.R.J., 2017. The social and economic value of cultural ecosystem services provided by urban forests in North America: A review and suggestions for future research. Urban. For. Urban. Green. 25, 103–111. https://doi.org/10.1016/j.ufug.2017.05.005.
Nesbitt, L., Meitner, M.J., Girling, C., Sheppard, S.R.J., Lu, Y., 2019. Who has access to urban vegetation? A spatial analysis of distributional green equity in 10 US cities. Landsc. Urban. Plan. 181, 51–79. https://doi.org/10.1016/J.LANDURBPLAN.2018.08.007.
Nielsen, A.B., Östberg, J., Delshammar, T., 2014. Review of Urban Tree Inventory Methods Used to Collect Data at Single-Tree Level. Arboric. & Urban. For. (AUF) 40 (2), 96–111. https://doi.org/10.48044/JAUF.2014.011.
Nitoslawski, S.A., Galle, N.J., van den Bosc, C.K., Steenberg, J.W.N., 2019. Smarter ecosystems for smarter cities? A review of trends, technologies, and turning points for smart urban forestry. Sustain. Cities Soc. 51, 101770. https://doi.org/10.1016/J.SCS.2019.101770.
Nowak, D.J., Greenfield, E.J., 2018. Declining urban and community tree cover in the United States. Urban. For. & Urban. Green. 32, 32–55. https://doi.org/10.1016/J.UFUG.2018.03.006.
Nowak, David J., Maco, Scott, Binkley, Mike, 2018. i-Tree: Global tools to assess tree benefits and risks to improve forest management. Arboric. Consult. 51 (4), 10–13. ⟨https://research.fs.usda.gov/treesearch/57414⟩.
NRCAN, 2025. High. Resolut. Digit. Elev. Model. (HRDEM) - CanElevation Ser. - Open. Gov. Portal. ⟨https://open.canada.ca/data/en/dataset/957782bf-847c-4644-a757-e383c0057995⟩.
Olson, L.G., Coops, N.C., Moreau, G., Hamelin, R.C., Achim, A., 2025. The assessment of individual tree canopies using drone-based intra-canopy photogrammetry. Comput. Electron. Agric. 234, 110200. https://doi.org/10.1016/J.COMPAG.2025.110200.
Parmehr, E.G., Amati, M., Taylor, E.J., Livesley, S.J., 2016. Estimation of urban tree canopy cover using random point sampling and remote sensing methods. Urban. For. & Urban. Green. 20, 160–171. https://doi.org/10.1016/J.UFUG.2016.08.011.
Pesaresi, M., Politis, P., 2023a. GHS-BUILT-H R2023A - GHS building height, derived from AW3D30. SRTM30, and Sentinel2 composite (2018). European Commission, Joint Research Centre (JRC) [Dataset].
Pesaresi, M., Politis, P., 2023b. GHS-BUILT-S R2023A - GHS built-up surface grid. derived from Sentinel2 composite and Landsat, multitemporal (1975-2030). European Commission, Joint Research Centre (JRC) [Dataset].
Pesaresi, M., Politis, P., 2023c. GHS-BUILT-V R2023A - GHS built-up volume grids derived from joint assessment of Sentinel2, Landsat, and global DEM data, multitemporal (1975-2030). European Commission, Joint Research Centre (JRC) [Dataset].
Rudin, C., 2019. Stop explaining black box machine learning models for high stakes decisions and use interpretable models instead. Nat. Mach. Intell. 1 (5), 206–215. https://doi.org/10.1038/S42256-019-0048-X.
Schindler, M., Schindler, J., 2025. Understanding street tree inequities: The interrelation of urban layout and socio-economics. Urban. For. & Urban. Green. 107 (2), 128765. https://doi.org/10.1016/j.ufug.2025.128765.
Selbig, W.R., Loheide, S.P., Shuster, W., Scharenbroch, B.C., Coville, R.C., Kruegler, J., Avery, W., Haefner, R., Nowak, D., 2022. Quantifying the stormwater runoff volume reduction benefits of urban street tree canopy. Sci. Total. Environ. 806, 151296. https://doi.org/10.1016/J.SCITOTENV.2021.151296.
Selim, S., Dönmez, B., Kilçik, A., 2023. Determination of the optimum number of sample points to classify land cover types and estimate the contribution of trees on ecosystem services using the I-Tree Canopy tool. Integr. Environ. Assess. Manag. 19 (3), 726–734. https://doi.org/10.1002/IEAM.4704.
Steenberg, J.W.N., Ristow, M., Duinker, P.N., Lapointe-Elmrabti, L., MacDonald, J.D., Nowak, D.J., Pasher, J., Flemming, C., Samson, C., 2023. A national assessment of urban forest carbon storage and sequestration in Canada. Carbon Balance Manag. 18 (1), 1–13. https://doi.org/10.1186/S13021-023-00230-4.
Strobl, C., Boulesteix, A.L., Kneib, T., Augustin, T., Zeileis, A., 2008. Conditional variable importance for random forests. BMC Bioinforma. 9 (1), 307. https://doi.org/10.1186/1471-2105-9-307.
Teixeira, F.Z., Printes, R.C., Fagundes, J.C.G., Alonso, A.C., Kindel, A., 2013. Canopy bridges as road overpasses for wildlife in urban fragmented landscapes. Biota Neotrop. 13 (1), 117–123. https://doi.org/10.1590/S1676-06032013000100013.
Terrestrial Ecozones of Canada - Open Government Portal. (n.d.). Retrieved August 13, 2025, from ⟨https://open.canada.ca/data/en/dataset/7ad7ea01-eb23-4824-bccc-66adb7c5bdf8⟩.
Tolan, J., Yang, H.I., Nosarzewski, B., Couairon, G., Vo, H.V., Brandt, J., Spore, J., Majumdar, S., Haziza, D., Vamaraju, J., Moutakanni, T., Bojanowski, P., Johns, T., White, B., Tiecke, T., Couprie, C., 2024. Very high resolution canopy height maps

from RGB imagery using self-supervised vision transformer and convolutional decoder trained on aerial lidar. Remote. Sens. Environ. 300. https://doi.org/10.1016/j.rse.2023.113888.
Tollefson, J., 2025. Google AI model mines trillions of images to create maps of Earth ‘at any place and time. Nature. https://doi.org/10.1038/D41586-025-02412-1;SUBJMETA.
Tucker, C.J., 1979. Red and Photographic Infrared l,lnear Combinations for Monitoring Vegetation. REMOTE Sens. Environ. 8.
USGS. (2019). Landsat 8 (L8) Data Users Handbook.
Vogeler, J.C., Braaten, J.D., Slesak, R.A., Falkowski, M.J., 2018. Extracting the full value of the Landsat archive: Inter-sensor harmonization for the mapping of Minnesota forest canopy cover (1973-2015). Remote. Sens. Environ. 209, 363–374. https://doi.org/10.1016/j.rse.2018.02.046.
Wright, M.N., Ziegler, A., 2017. ranger: A Fast Implementation of Random Forests for High Dimensional Data in C++ and R. J. Stat. Softw. 77 (1), 1–17. https://doi.org/10.18637/JSS.V077.I01.
Zhang, G., Lu, Y., 2012. Bias-corrected random forests in regression. J. Appl. Stat. 39 (1), 151–160. https://doi.org/10.1080/02664763.2011.578621.
Zhao, Y., Gong, P., 2024. Optimal site selection strategies for urban parks green spaces under the joint perspective of spatial equity and social equity. Front. Public. Health 12, 1310340. https://doi.org/10.3389/FPUBH.2024.1310340/BIBTEX.
Ziter, C.D., Pedersen, E.J., Kucharik, C.J., Turner, M.G., 2019. Scale-dependent interactions between tree canopy cover and impervious surfaces reduce daytime urban heat during summer. Proc. Natl. Acad. Sci. USA 116 (15), 7575–7580. https://doi.org/10.1073/pnas.1817561116.